Nanometer-scale organization of the alpha subunits of the receptors for IL2 and IL15 in human T lymphoma cells

Bärbel I. de Bakker[1], Andrea Bodnár[2], Erik M. H. P. van Dijk[1], György Vámosi[2], Sándor Damjanovich[2,3], Thomas A. Waldmann[4], Niek F. van Hulst[5,6], Attila Jenei[3,*] and María F. Garcia-Parajo[6,7,*]

[1]Applied Optics group, Faculty of Science and Technology, MESA+ Research Institute for Nanotechnology, University of Twente, PO Box 217, 7500 AE Enschede, The Netherlands
[2]Cell Biology and Signaling Research Group of the Hungarian Academy of Sciences, Research Center for Molecular Medicine, Medical and Health Science Center, University of Debrecen, PO Box 39, 4032 Debrecen, Hungary
[3]Department of Biophysics and Cell Biology, Research Center for Molecular Medicine, Medical and Health Science Center, University of Debrecen, PO Box 39, 4012 Debrecen, Hungary
[4]Metabolism Branch/National Cancer Institute, National Institutes of Health, Bethesda MD 20892-1374, USA
[5]ICFO-Institut de Ciències Fotòniques, 08860 Barcelona, Spain
[6]ICREA-Institució Catalana de Recerca i Estudis Avançats, 08010 Barcelona, Spain
[7]IBEC-Institut de Bioenginyeria de Catalunya and CIBER-BNN, Josep Samitier 1-5, Barcelona 08028, Spain
*Authors for correspondence (e-mail: jenei@jaguar.dote.hu; mgarcia@pcb.ub.es)

Summary

Interleukin 2 and interleukin 15 (IL2 and IL15, respectively) provide quite distinct contributions to T-cell-mediated immunity, despite having similar receptor composition and signaling machinery. As most of the proposed mechanisms underlying this apparent paradox attribute key significance to the individual α-chains of IL2 and IL15 receptors, we investigated the spatial organization of the receptors IL2Rα and IL15Rα at the nanometer scale expressed on a human CD4^{+} leukemia T cell line using single-molecule-sensitive near-field scanning optical microscopy (NSOM). In agreement with previous findings, we here confirm clustering of IL2Rα and IL15Rα at the submicron scale. In addition to clustering, our single-molecule data reveal that a non-negligible percentage of the receptors are organized as monomers. Only a minor fraction of IL2Rα molecules reside outside the clustered domains, whereas ~30% of IL15Rα molecules organize as monomers or small clusters, excluded from the main domain regions.

Interestingly, we also found that the packing densities per unit area of both IL2Rα and IL15Rα domains remained constant, suggesting a 'building block' type of assembly involving repeated structures and composition. Finally, dual-color NSOM demonstrated co-clustering of the two α-chains. Our results should aid understanding the action of the IL2R-IL15R system in T cell function and also might contribute to the more rationale design of IL2R- or IL15R-targeted immunotherapy agents for treating human leukemia.

Supplementary material available online at
http://jcs.biologists.org/cgi/content/full/121/5/627/DC1

Key words: Near-field scanning optical microscopy (NSOM), Interleukin receptors IL2R, IL15R, Single-molecule detection, nanometer-scale membrane organization

Introduction

Interleukin 2 (IL2) and interleukin 15 (IL15) are substantially involved in controlling T cell homeostasis and function (Waldmann et al., 2001). Their respective receptors comprise three distinct components: the α-chains are cytokine specific, whereas the β- and γc-subunits are utilized by both IL2 and IL15. In addition, the so-called common γc-chain is a component of a series of other cytokine receptors, these being members of the γc cytokine receptor family (IL4, IL7, IL9, IL21) (Nakamura et al., 1994; Nelson and Willerford, 1998; Fehniger and Caligiuri, 2001; Tagaya et al., 1996). As a result of combining the various subunits, several forms of receptor complexes with different affinities to the interleukins might exist at the cell surface. The trimeric receptor complexes (αβγc) of both IL2 and IL15 have similar high affinities for their ligands (K_d 10^{-11} M). The βγc heterodimer has an intermediate affinity for both cytokines (K_d 10^{-9} M). In contrast to IL2 receptor α (IL2RA, hereafter referred to as IL2Rα), which on its own binds to IL2 with very low affinity (K_d 10^{-8} M), IL15 receptor α (IL15RA, hereafter referred to as IL15Rα) is capable of binding to IL15 with a high affinity matching that of the trimeric IL15R (Lin et al., 1995).

Heterodimerization of the intracellular domains of the β- and γc-chains is crucial for one set of signaling events shared by both cytokines (Nakamura et al., 1994; Fehniger et al., 2001). In this case, IL2 and IL15 activate similar signaling pathways involving Janus kinase (JAK1/JAK3)-assisted tyrosine phosphorylation of downstream signaling molecules (e.g. signal transducer and activator of transcription molecules STAT3 and STAT5) (Lin et al., 1995). As IL2Rα does not possess signaling capacity, IL2-induced signals are transmitted solely by the IL2Rαβγc heterotrimeric or the βγc heterodimeric forms of the IL2R complexes and utilize the Jak-STAT-related pathways. By contrast, it appears that IL15 can stimulate additional signaling pathways employing IL15Rα but not requiring the expression of the βγc heterodimer (Bulanova et al., 1995).

As a consequence of utilising shared receptor subunits and common signaling elements, IL2 and IL15 induce similar cellular responses in many cases (Waldmann et al., 2001). Among others, they both stimulate the proliferation of several T cell subsets and facilitate the induction of cytolytic effector T cells (Grabstein et al., 1994; Waldmann and Tagaya, 1999). However, they can also exhibit quite distinct and contrasting contributions to T-cell-mediated immunity. Through its central role in activation-induced cell death (AICD), IL2 is involved in peripheral tolerance to self-reactive T cells. IL15, by contrast, inhibits IL2-mediated AICD (Marks-Konczalik et al., 2000) and stimulates the persistence of CD8^{+} memory T cells (Ku et al., 2000). Many explanations have been proposed to resolve this apparent contradiction. It has been shown previously that, in the early phase of the immune response, IL15Rα expressed on antigen-presenting cells (e.g. monocytes, dendritic cells) can present the tightly associated IL15 in trans to a cytokine-responsive second cell (e.g. natural killer or memory T cell) expressing only the β and γ$_c$ chains (Dubois et al., 2002). By contrast, IL2 mainly acts as a soluble factor binding to receptor complexes on a single T cell. The existence of the aforesaid βγ$_c$-independent signaling routes by IL15Rα alone is another possible explanation for the diverse outcomes of biological responses invoked by IL15 and IL2 (Bulanova et al., 2001).

On cells expressing all the elements of the IL2R-IL15R system, the diversity of downstream signaling might originate from the different molecular interactions of the two α chains. However, our recent confocal laser scanning microscopy (CLSM) and fluorescence resonance energy transfer (FRET) experiments revealed the physical proximity of IL2Rα and IL15Rα as well as their association with the β- and γ$_c$-subunits and with major histocompatibility complex (MHC) glycoproteins in lipid rafts of human T lymphoma/leukemia cells, indicating a considerable similarity between the direct molecular environment of the two α-chains (Vámosi et al., 2004). However, it can be assumed that cytokine-specific modulation of subunit assembly within lipid rafts, and, as a result, the alteration of receptor affinity and/or conformation of the recruited signaling elements, might explain the distinct actions of IL2 and IL15. Indeed, based on our FRET data, a heterotetrameric model of the IL2-IL15R complex could be generated, where binding of IL2 or IL15 causes the formation of the appropriate high-affinity receptor trimer (αβγ$_c$), while the 'unused' α-chain moves away from the site of cytokine-receptor interaction (Vámosi et al., 2004). A distinct involvement of FK506-binding proteins 12 and 12.6 in IL2- versus IL15-mediated T cell responses has also been reported (Dubois et al., 2003).

Most of the proposed mechanisms that might underlie the divergence in IL2 and IL15 signaling are based on the unique α-chains of the two cytokines. Therefore, we decided to investigate the organization of IL2Rα and IL15Rα on a human CD4^{+} leukemia T cell line, Kit 225 FT7.10, at high spatial resolution using near-field scanning optical microscopy (NSOM). NSOM is a technique based on lensless optical imaging that provides simultaneous optical and topographic lateral resolution beyond the diffraction limit of light (de Lange et al., 2001; Ianoul et al., 2005). The technique is based on local excitation of the sample using a sub-wavelength light source that is then raster-scanned over the surface. The lateral resolution is limited to the dimension of the aperture (typically ~70 nm), whereas the axial resolution is defined by the diffraction of the evanescent field emanating from the aperture (<50 nm), resulting in an overall reduction of the illumination volume by a factor of >100 below the diffraction limit. As such, the technique is

particularly suitable for investigating the distribution of membrane components on the cell surface with nanometer precision and single-molecule detection sensitivity (de Lange et al., 2001; Koopman et al., 2004).

As an extension of our previous CLSM experiments reporting on the lateral distribution and colocalization of IL2Rα and IL15Rα at the submicron scale (Vámosi et al., 2004; Vereb et al., 2000), we now provide detailed analysis at a finer spatial scale, confirming clustering of IL2Rα and IL15Rα on the cell membrane. Moreover, the single-molecule-detection sensitivity of our NSOM technique also provides insight into the inner structure of these domains and has allowed us to derive quantitative analysis of the packing densities and intermolecular distances between their components. Furthermore, information on the fraction of proteins residing inside or outside the domain regions has been obtained. Finally, simultaneous excitation of both IL2Rα and IL15Rα with the same NSOM probe showed co-clustering at the nanometer scale, supporting previous FRET and CLSM observations.

Results

High-resolution NSOM imaging of IL15Rα and IL2Rα in the plasma membrane of FT7.10 cells

In the first set of experiments, the lateral organization of IL15Rα and IL2Rα was investigated independently, that is in different cells, using specific Cy5-tagged monoclonal antibodies (mAbs) to target the proteins. Fig. 1 shows a complete measurement sequence starting with a bright-field image of two fixed T cells (Fig. 1A) and finishing with a high-resolution NSOM image (Fig. 1C,D) mapping the
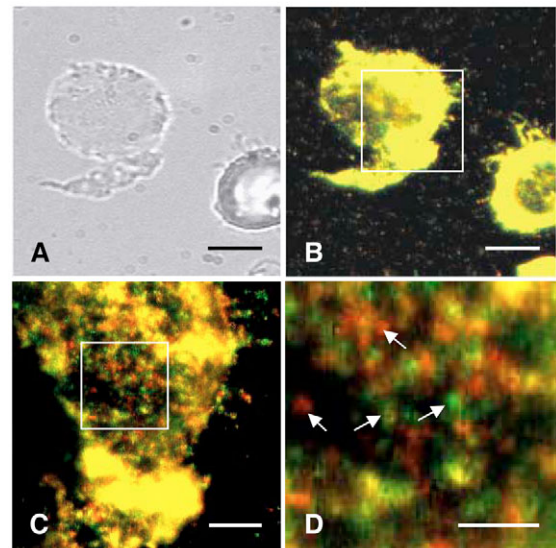

Fig. 1. (A) Bright-field image of fixed Kit 225 FT7.10 cells labeled with Cy5-conjugated antibodies against IL15Rα. Bar, 5 μm. (B) Confocal fluorescence image of the same sample area as in A. Bar, 5 μm. (C) NSOM image of the area highlighted in B, and magnified in D, demonstrating the increased spatial resolution and sensitivity of the technique as compared with that of the confocal method. The fluorescence signal on the images is color coded according to the detected polarization, red for 0° channel and green for 90° channel. The arrows in D point to some single-molecule spots. Individual molecules are identified by their unique dipole emission – that is, red and green color-coding. The yellow color of most fluorescent spots results from adding multiple molecules with random in-plane orientation (combination of red and green) in one spot and thus reflects the clustering of receptors on the cell membrane. Bars, 2 μm (C); 1 μm (D).

distribution of IL15Rα in the plasma membrane. From the confocal image shown in Fig. 1B, it is apparent that IL15Rα is distributed over the whole cell. Fig. 1C shows the NSOM image obtained from the region highlighted in Fig. 1B, while Fig. 1D shows with greater detail the distribution of individual receptors on the membrane with a spatial resolution of ~90 nm. The high spatial resolution and surface sensitivity of NSOM provides greater detail than confocal microscopy; for example, fluorescence spots arising from single molecules (or small clusters) are readily detected on the cell surface (indicated in Fig. 1D). Additionally, fluorescent patches were also observed, indicating the presence of larger-scale clusters of IL15Rα on FT7.10 cells.

The spatial organization of IL2Rα was also studied by NSOM in a manner similar to that used for IL15Rα. Fig. 2 shows a combined image of four spatially different NSOM measurements mapping the entire distribution of IL2Rα in the plasma membrane of an FT7.10 cell. Supplementary material Fig. S1 shows the four independent NSOM images. Just like IL15Rα, the cell membrane exhibits two types of protein coverage – clustered regions of IL2Rα displayed as bright fluorescent patches, as well as low-coverage areas containing single-molecule fluorescent spots with a size determined by the NSOM aperture and indicating the presence of only a few proteins.

Intensity analysis of the IL2Rα and IL15Rα domains

To obtain in-depth information about the extent of similarity between the organization of IL2Rα and IL15Rα in the plasma membrane, we performed detailed quantitative analysis of the domain properties for both types of proteins. All fluorescent spots in the NSOM images of IL2Rα and IL15Rα were analyzed in terms of their intensity, as described in the Materials & Methods section. Fig. 3A,B show the intensity distributions of individual fluorescence spots of IL2Rα or IL15Rα extracted from cells labeled with Cy5-tagged 7G7 B6 or Cy5-tagged 7A4 24 mAbs, respectively. Some of the fluorescent spots were attributed to the emission of individual molecules, as they showed one-step photobleaching and a unique
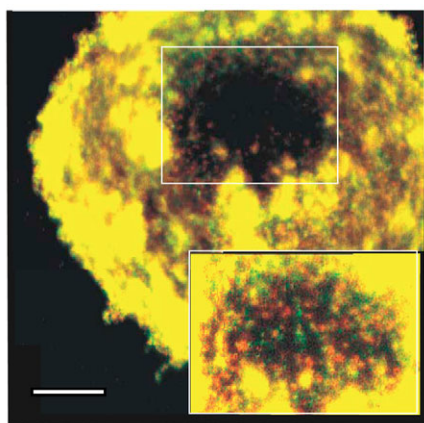

Fig. 2. Composite of four near-field fluorescence measurements performed on a Cy5-IL2Rα-labeled FT7.10 cell mapping the full distribution of the receptor on the membrane. The color coding of the image is the same as in Fig. 1. A compromise in image contrast accounts for the effect that the low-intensity spots in the middle of the cell are not clearly visible. The inset shows the central part of the cell with a different imaging contrast, revealing the presence of individual molecules (green and red spots corresponding to single dipole emission). Bar, 2 μm. The four independent NSOM images are shown in supplementary material Fig. S1.
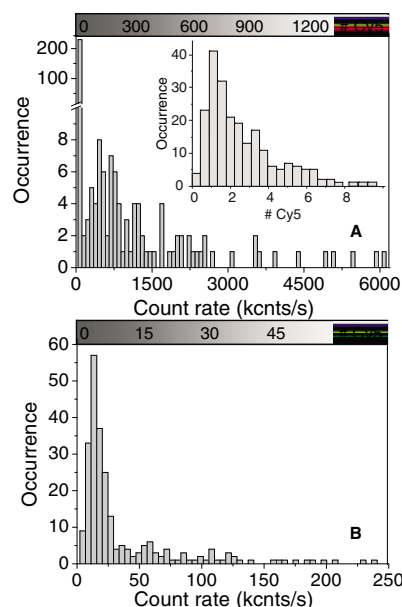

Fig. 3. Intensity distribution in terms of the fluorescence count rate and a normalized axis containing the number of Cy5 molecules for all images analyzed (see text for details) for (A) Cy5-IL2Rα and (B) Cy5-IL15Rα. The inset in A shows more accurately the low-intensity part of the distribution.

emission dipole moment (data not shown), signatures that are characteristic of single-molecule fluorescence detection (van Hulst et al., 2000). A typical count rate for individual Cy5 molecules of ~4000 counts/second at the applied excitation intensity of 200 W/cm² was obtained. This value was used to normalize the intensity axis on the distributions shown in Fig. 3A,B and thus to obtain an estimate of the number of Cy5 molecules (and so the number of α-chains) contained in each domain.

Interestingly, the intensity distribution of IL2Rα showed two main contributions: a narrow low-intensity part peaking at ~1.5 Cy5 molecules (see also the inset in Fig. 3A) and a second broader-intensity distribution peaking at ~130 Cy5 molecules per domain but extending up to more than 1000 Cy5 molecules per domain (Fig. 3A). These distinct distributions were, in fact, already apparent in Fig. 2, where both high-intensity patches as well as low-intensity spots were mapped. Making the reasonable assumptions that no unbound Cy5 molecules are present on the cell surface and that a one-to-one antibody-to-protein ratio is used, the lower-intensity distribution can then be attributed to individual IL2Rα proteins. From the analysis of seven different NSOM images, ~1.4±1.1% of IL2Rα subunits are spatially distributed as monomers, whereas the remainder are clustered in domains. Similarly, the intensity distribution of IL15Rα also shows two populations, although positioned much more closely to each other. The peak values of the two populations are ~3 and ~15 Cy5 molecules per domain (Fig. 3B). Considering that the dye-protein labeling efficiency for IL15Rα is ~3 (see Materials and Methods), the lower-intensity peak corresponds most probably to monomeric IL15Rα and accounts for ~29±14% of the overall IL15Rα population, whereas the remaining subunits are organized as clusters on the cell membrane. Furthermore, the peak values of the intensity distributions corresponding to clustering indicated that IL2Rα and IL15Rα domains consist typically of ~90 and ~5 proteins, respectively. These results are fully in line with our previous flow cytometry data
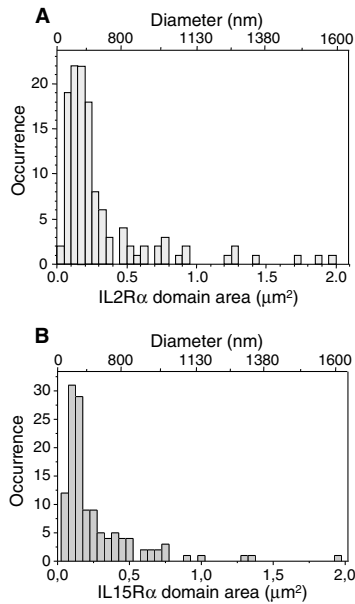
Fig. 4. Domain area/size distributions for domains of IL2Rα (A) and IL15Rα (B) for all images analyzed. For convenience, both the occupied domain area (μm^2) and the corresponding domain diameter are indicated on the horizontal axis of both distributions.

Fig. 5. (A) Correlation plots between domain area and the number of receptors contained in each domain for IL2Rα (□) and IL15Rα (○) for all images analyzed. The dotted lines are the lines of best fit to the correlation plots and suggest a constant packing density of both receptors on the cell membrane. (B) Distribution of the estimated intermolecular separations of IL2Rα and IL15Rα within each individual domain for all images analyzed.

reporting on the significantly higher expression of IL2Rα in comparison with IL15Rα on FT7.10 cells (Vámosi et al., 2004).

Size and packing density of the IL2Rα and IL15Rα domains

We next focused on the physical size of the IL2Rα and IL15Rα domains. The size of a domain was defined as the area within a contour line drawn by software around twice the intensity of the background level. The distribution of the occupied areas and the sizes of the IL2Rα and IL15Rα domains are shown in Fig. 4. The typical area of the IL2Rα domains was 0.15 μm^2, corresponding to a diameter of ~450 nm. Similarly, the IL15Rα domain areas were typically 0.10 μm^2, corresponding to a diameter of ~360 nm. Interestingly, while the domain sizes for IL2Rα and IL15Rα were found to be rather similar to each other, their intensities differed by more than one order of magnitude, as disclosed by the fluorescence intensity analysis (see above), reflecting a different packing density of both receptor subunits on the membrane.

To elucidate the domain packing density, we correlated the intensity versus the area of all individual domains (Fig. 5A). The correlation plot for IL2Rα and IL15Rα follows a linear dependence, indicating that the domains have a constant molecular packing density regardless of the specific domain size. In the case of the IL2Rα domains, the slope of the curve renders a molecular density of 1350 IL2Rα/μm^2, indicating that on average one IL2Rα molecule is present in an area of 27×27 nm^2. By contrast, IL15Rα domains have a molecular density of 120 IL15Rα/μm^2, indicating one IL15Rα molecule per area of 92×92 nm^2. Thus, IL2Rα domains are approximately ten times denser than IL15Rα domains.

We also estimated the IL2Rα and IL15Rα intermolecular separations for each domain, assuming a random arrangement for both types of α chains within the domains. The resultant distributions are displayed in Fig. 5B. Clearly, two distinct distributions for molecular distances within IL2Rα and IL15Rα are obtained. The peak of the distributions lies at ~14 nm and ~50 nm
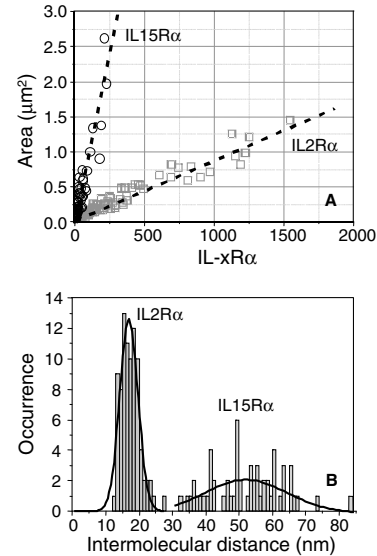
for the IL2Rα and IL15Rα domains, respectively. These values correspond approximately to the formula $0.5/\sqrt{a}$, where a is the slope derived from Fig. 5B. However, it should be noted that our previous FRET data showed at least partial homodimerization/oligomerization of both IL2Rα and IL15Rα in FT7.10 cells, which necessitates a refinement of the above picture (see Discussion).

Nanometer-scale colocalization of IL2Rα and IL15Rα domains

The relative spatial arrangement of IL2Rα and IL15Rα domains in the plasma membrane of FT7.10 cells was also investigated using dual-color excitation-detection NSOM. In good accordance with our previous results obtained using FRET and CLSM (Vámosi et al., 2004), high-resolution NSOM images of the two α-chains targeted with 7A4 24 (IL15Rα) and 7G7 B6 (IL2Rα) mAbs carrying
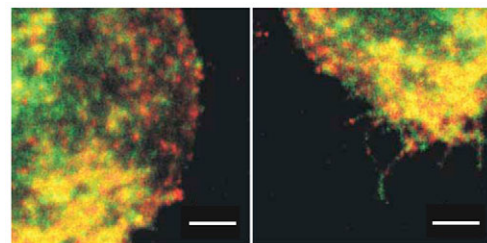

Fig. 6. High-resolution dual-color excitation-detection NSOM of two different cells reflecting nanometer-scale spatial colocalization of IL2Rα (labeled with Alexa-Fluor-488-conjugated 7G7-B6 mAb) and IL15Rα (labeled with Cy5-conjugated 7A4 24 mAb) on the cell membrane. Here the pseudo-color scale refers to spectral contrast, with Alexa-Fluor-488 emission shown in green, whereas Cy5 emission is shown in red. The yellow color indicates colocalization of Alexa-Fluor-488 and the Cy5 signal. The degree of colocalization has been calculated using the Pearson's correlation coefficient over ten different cells imaged with NSOM (see Materials and Methods for details). Bars, 1 μm.

different fluorophores (Alexa-Fluor-488 and Cy5, respectively) indicated considerable colocalization between IL2Rα and IL15Rα domains (Fig. 6). Hence, the correlation coefficient over ten different imaged cells rendered a value of 0.40±0.17 (see Materials and Methods). For non-domain regions, a much lower correlation (*C*) value was found, i.e. *C*=0.17±0.09. To exclude any possible artefact due to cell autofluorescence and/or differences in labeling efficiency, we also measured the correlation coefficient from images obtained from cells labeled with Alexa-Fluor-488–7G7-B6 and Cy5–7A4-24. The values obtained remained broadly the same as before, being 0.48±0.15 for the domain regions and 0.23±0.14 for the non-domain regions.

Discussion

Although IL2 and IL15 share two receptor subunits and many functions, especially in innate immunity, they provide at times distinct and contrasting contributions to T-cell-mediated immune responses. A number of molecular mechanisms could underlie this bifurcation of signaling capacities, most of them attributing key significance to the distinct α-chains of the two receptor types (Waldmann et al., 2001; Vámosi et al., 2004). Recent evidence suggests that IL15Rα on its own can mediate signals evoked by IL15 without the contribution of the βγ$_c$ heterodimer (Bulanova et al., 2001). It was also demonstrated that cells bearing IL15Rα can present the tightly associated IL15 in trans to other cells (e.g. CD8+ T cells) expressing only the β- and γ$_c$-chains (Dubois et al., 2002). Membrane-bound IL15 presented in trans to target cells was found to lead to more prolonged and persistent activation of the target cells (Sato et al., 2007; Budagian et al., 2006). On cells where all the elements of the IL2R-IL15R system are coexpressed in the same membrane domains, the proximity of the distinct α-chains might alter the conformation of the β- and γ$_c$-subunits in distinct ways, thereby also modulating the nature of downstream signals mediated by IL2 or IL15.

Our major focus has been to investigate the lateral organization and topological relationship of IL2Rα and IL15Rα in the plasma membrane of a CD4+ human leukemia T cell line Kit 225 FT7.10. By using CLSM on FT7.10 cells, we have recently shown that the four subunits of the IL2R-IL15R system strongly colocalize with GM1-rich membrane microdomains (lipid rafts) (Vámosi et al., 2004). Furthermore, our FRET experiments suggested that IL2Rα and IL15Rα associate with each other as well as with the β- and γ$_c$-chains. Here, we have further analyzed the membrane topology of IL2Rα and IL15Rα on FT7.10 cells by NSOM. The high spatial resolution provided by NSOM bridges the gap between the resolutions of CLSM and FRET experiments (~300 nm and 1-10 nm, respectively). In addition, NSOM allows single-molecule detection even in densely packed areas. As such, the use of NSOM combined with single-molecule detection sensitivity has provided new insights into the organization of these receptors.

Although clustering of IL2Rα and IL15Rα at the submicron scale has also been inferred by confocal microscopy (Vámosi et al., 2004; Vereb et al., 2000), direct analysis of cluster size and density has been lacking so far. Here, we have directly observed domains of IL2Rα and IL15Rα by fluorescent means. Our data confirmed the existence of IL2Rα domains of typically 450 nm in diameter (Fig. 4A), in good agreement with previous CLSM and electron-microscopy studies (Vereb et al., 2000). We also observed clustering of IL15Rα at this hierarchical level in the plasma membrane of FT7.10 cells. IL15Rα domain sizes were similar to those of IL2Rα domains (~360 nm diameter; Fig. 4B). Nevertheless, the number

of α-chains in their respective domains differed by more than one order of magnitude, as disclosed by the fluorescence intensity analysis of individual fluorescence spots. The latter is in good agreement with flow cytometry measurements showing that the total number of IL2Rα subunits expressed by FT7.10 cells is ~5-10 fold higher than that of the IL15Rα (Vámosi et al., 2004). Finally, our current NSOM experiments confirmed the colocalization of IL2Rα- and IL15Rα-containing membrane domains (Fig. 6). On the basis of our previous CLSM and FRET data, the formation and colocalization of IL2Rα and IL15Rα domains presumably takes place in lipid rafts of FT7.10 cells and also contains other elements of the IL2R-IL15R system (Vámosi et al., 2004; Vereb et al., 2000; Matkó et al., 2002).

Interestingly, we found that the packing densities (i.e. the number of α-chains per unit area) of both IL2Rα and IL15Rα domains were constant, irrespective of their sizes (Fig. 5A). This result might imply that the domains are assembled from 'building blocks' with repeated structures and composition. On the basis of FRET and CLSM studies, we previously suggested the existence of 'supercomplexes' formed by the elements of the IL2–IL15R system as well as MHC (and intercellular adhesion molecule ICAM-1) molecules in lipid rafts of T cells (Vámosi et al., 2004). These supercomplexes could be potential candidates for the building elements of the domains. It is probable that the constant molecular densities of IL2Rα and IL15Rα domains are optimized for their signaling function and could thus allow signaling with similar strength for all signaling domains. It is important to mention that not all the cell-surface receptors are organized in this way. For instance, the pathogen recognition receptor DC-SIGN also forms domains at the submicron scale on immature dendritic cells, but with a rather heterogeneous packing density (de Bakker et al., 2007). It has been postulated recently that, owing to its substantial glycosylation, the structure of IL2Rα is relatively rigid, forming a notable entropic barrier preventing the formation of the quaternary receptor complex (Chirifu et al., 2007). We hypothesize that association with MHC glycoproteins might compensate for this entropic barrier. The latter is supported by the fact that association of the IL2R complex with MHC class I was observed previously in different human T cell types, including cell lines of T lymphoma origin as well as lymphocytes from healthy donors and colorectal carcinoma patients (Matkó et al., 2002; Bene et al., 2007).

Assuming a random distribution of the α-chains, the average intermolecular separation between the mutual IL2Rα and IL15Rα subunits within the domains was ~14 and ~50 nm, respectively (Fig. 5B). At the same time, our former FRET experiments indicated homodimeric/oligomeric molecular association of both IL2Rα and IL15Rα in the plasma membrane of FT7.10 cells (Vámosi et al., 2004). This changes the situation such that instead of (or in addition to) single entities, presumably, dimers (or higher-order oligomers) of the α-chains are distributed randomly throughout the domains, which also could produce a constant packing density (necessarily with different mutual separations). This probably holds true for IL2Rα, but we cannot exclude that dimerization/oligomerization of IL15Rα is restricted to the non-domain areas (see below).

In addition to clustering at the submicron scale, we also observed a minor fraction (~1%) of IL2Rα located in the cell membrane as small aggregates consisting of only a few proteins or even monomers. Previous FRET experiments had already hinted at the existence of a minor fraction of IL2Rα subunits associated with transferrin receptors (TrfRs) (Matkó et al., 2002), which are excluded from lipid rafts (Harder et al., 1998). Our findings

strongly indicate that we directly observed IL2Rα proteins associated with the TrfR. In contrast to IL2Rα, a considerable portion (~30%) of IL15Rα subunits was found to reside outside the domains and appeared in smaller clusters or even as monomers. Although we cannot completely exclude the possibility that this high percentage of IL15Rα outside the domains is a consequence of overexpression, the absence of IL2Rα molecules outside the domains argues against the possibility that artefacts are generated by overexpression of receptors. Notably, the extent of colocalization with IL2Rα was significantly lower for the 'non-domain' IL15Rα molecules than that for the clustered molecules. It is conceivable that this relatively large fraction of IL15Rα could be responsible for those functions of IL15 that are mediated by the interaction of IL15 with IL15Rα alone, including βγc-independent signaling routes or trans-presentation of IL15 to neighboring cells.

Recent crystallographic data have revealed considerable similarities in the topologies of the quaternary IL15-IL15R and IL2-IL2R complexes (Chirifu et al., 2007). It has been suggested that IL2, like IL15, might be capable of being presented in trans by IL2Rα on one cell to another cell expressing the β and the γc chains. Indeed, it has been shown previously that native IL2Rα-bearing cells augmented the proliferative response evoked by IL2 in ex vivo large granular lymphocytic leukemia cells expressing the β and γc chains but lacking the α-subunits of the IL2 receptor (Eicher and Waldmann, 1998). Taking into account the rather low affinity and high off-rate of IL2Rα for IL2 (Liparoto et al., 2002), this process could be prominent only in cells displaying highly elevated level of the α chains (e.g. numerous T lymphoma/leukemia cells, including the Kit 225 cells used in this study). Accumulation of IL2Rα into domains disclosed by our current and previous experiments (Vámosi et al., 2004) could further increase the avidity of trans-interactions by concentrating a large number of IL2Rα molecules in restricted areas and therefore enhancing the density of IL2-IL2Rα complexes.

Taken together, our experiments provide direct data on the size and finer structure of the large-scale (submicron size) domains of IL2Rα and IL15Rα revealed previously by confocal microscopy. Moreover, we demonstrate that, in addition to the aforementioned domains, IL15Rα (and a minor fraction IL2Rα) also exists as monomers or small clusters in the plasma membrane of T cells. Although our previous confocal and FRET experiments did not show evidence for rearrangement of IL2 and IL15 receptors on the membrane after cytokine stimulation and/or ligand binding, NSOM could potentially bring further insight into their relative organization on an intermediate spatial scale (50-200 nm). Similarly, dual-color NSOM experiments, based on the ones described here, could be performed with the aim of mapping the potential association of these receptors with lipid rafts and/or with MHC molecules. Our current and earlier data on the spatial organization of the IL2 and IL15 receptors should contribute to our understanding of the regulation of T cell functions by these cytokines. The importance of this question is also underlined by the progress towards IL2R- and IL15R-targeted immunotherapy of human leukemia, autoimmune disorders and HTLV-I-associated diseases (Waldmann et al., 2001).

Materials and Methods
Cell culture
Kit225 FT7.10 is a human T-cell leukaemia virus (HTLV)-nonexpressing, cytokine-dependent (IL2 or IL15) human adult T lymphoma cell line with a helper/inducer phenotype derived from Kit225 cells (Hori et al., 1987). FT7.10 cells express constitutively all subunits of the IL2R-IL15R system (Vámosi et al., 2004). In addition

to the endogenous nonfunctional form of IL15Rα, manifesting a deletion of exons 3 and 4, FT7.10 cells have been transfected with the gene encoding the complete IL15Rα subunit together with an N-terminal FLAG tag. In agreement with our previous findings, cell-surface expression of the transfected IL15Rα was >tenfold higher than that of endogenous IL15Rα (Vámosi et al., 2004). The cell line was cultured in RPMI 1640 medium supplemented with 10% FBS, penicillin and streptomycin at 37°C, in a humidified 5% CO_2 atmosphere. It is important to note that the Kit225 FT7.10 cell line requires IL2 for its growth. Therefore, we also added 500 pM human recombinant IL2 to the medium every 48 hours. Cells cultured for 2 days in this medium were harvested, processed for the experiments and then analyzed, as explained below, with no extra IL2 being added before the experiments. This essentially means that the experiments were performed in an 'unliganded' state. The culture medium contained 800 μg/ml G418 (Gibco) in order to suppress the growth of nontransfected wild-type cells.

Monoclonal antibodies
IL2Rα was targeted with mAb 7G7 B6 (IgG2a) defining an epitope that does not compete with the cytokine-binding site (Rubin et al., 1985). IL15Rα was labeled with 7A4 24 (IgG2), recognizing both the transfected and the native deletion mutant population of IL15Rα (Dubois et al., 2002; Vámosi et al., 2004). The specificity of the antibodies was proven previously by using human cell lines positive or negative for their respective antigens (Dubois et al., 2002; Yang et al., 2003). Furthermore, our flow cytometric experiments failed to detect significant binding of isotype-matched antibodies (see supplementary material Figs S2 and S3). Aliquots of purified mAbs were conjugated with succinimidyl esters of Alexa-Fluor-488 (Molecular Probes) or Cy5 (Amersham Pharmacia) dyes, as described by Szöllösi et al. (Szöllösi et al., 1996) and Sebestyen et al. (Sebestyen et al., 2002). The dye-to-protein ratio was determined spectrophotometrically. The obtained ratios were: ~3 for Cy5–7A4-24 (IL15Rα), ~2 for Cy5–7G7-B6 (IL2Rα), ~3 for Alexa-Fluor-488–7A4-24 (IL15Rα) and ~1 for Alexa-Fluor-488–7G7-B6 (IL2Rα). The fluorescent antibodies retained their affinity according to competition with identical unlabeled antibodies. To avoid possible aggregation of the antibodies, they were centrifuged at 90,000 rpm, for 30 minutes before labeling.

Labeling cells with fluorescent markers
Freshly harvested cells were washed twice in ice-cold PBS (pH 7.4). The cell pellet was suspended in PBS ($0.5-1×10^6$ cells/50 μl) and incubated with 50 μg/ml fluorescent mAbs for 45 minutes on ice. The excess of mAbs was at least 30-fold above the K_d during the incubation. Special care was taken to keep the cells at an ice-cold temperature to avoid induced aggregation or internalization of interleukin receptors. After being washed with excess cold PBS, cells were layered onto a glass coverslip and fixed with 4% formaldehyde-PBS for 60 minutes on ice, and then were dehydrated in an ethanol series (Nagy et al., 2001).

Combined confocal and near-field scanning optical microscopy
The experiments were performed using a combined confocal–near-field optical microscope equipped with single-molecule detection sensitivity (Garcia-Parajó et al., 2005). In confocal mode, incoming circularly polarized light was reflected by a dichroic mirror and focused onto the sample using an oil-immersion objective (Olympus, 64×, 1.4 NA). In NSOM mode, the light was coupled into an Al-coated tapered fiber probe (single mode, λ=633 nm, Cunz, Frankfurt), with an end-face aperture of ~90 nm in diameter. The probe was kept in the near-field region of the sample (<10 nm) by means of shear-force feedback, providing simultaneously a topographic map of the sample surface while scanning (Koopman et al., 2004). A flipable mirror mount (Newfocus) enabled easy switching between excitation modes.

Single-color fluorescence experiments of Cy5-labeled proteins were performed using the 647 nm excitation line of an Ar-Kr laser at an excitation intensity of 200 W/cm². For dual-color experiments, samples were labeled simultaneously with Alexa-Fluor-488- and Cy5-conjugated mAbs against the two α-chains, avoiding possible FRET between the two fluorophores. For simultaneous excitation at 488 and 647 nm in the confocal mode, a dual-band dichroic mirror (XF2041, Omega Optical) was placed in the excitation path. The polarization and excitation intensities were adjusted independently before overlapping the two beams. Dual-color NSOM excitation was achieved by coupling the 488 nm and 647 nm lines (excitation power controlled independently for each beam) into the back-end of the fiber probe. The subwavelength aperture probe guarantees perfect overlay of the two different excitation wavelengths, without chromatic aberrations. On the detection side, the emitted fluorescence was collected by the objective and separated into two orthogonal polarization components by a broadband beam splitter (400-700 nm, Newport, Fountain Valley, CA) in the case of single-color experiments or into two spectrally separated channels for dual-color experiments and focused onto two avalanche photodiodes (SPCM-100, EG&G, Quebec) after appropriate filtering.

Cells were first screened for their overall structure and height, using the bright-field mode of the microscope. An area of typically 20×20 μm² from the selected cell was imaged in confocal mode with either single- or dual-wavelength excitation. Regions of interest (typically 5×5 μm²) were then imaged by NSOM using single- or dual-color excitation. The same NSOM aperture probe (~90 nm in diameter) was used in all experiments. In total, seven cells of the two different sample sets have

been investigated by performing 30 near-field measurements with single- and dual-wavelength excitation.

Image analysis

Unprocessed images were analyzed using custom-made software that determines the size and brightness of each fluorescent spot. In the case of single-molecule spots, their size was determined using the full-width-at-half-maximum (FWHM) of a two dimensional Gaussian fit to the intensity profile. In the case of domains, their size was defined as the area within a contour line drawn by software around twice the intensity of the background level. The brightness of each spot was defined as the background-corrected sum over all pixels within the FWHM for single-molecule spots or within a contour of twice the intensity of the background level for the larger fluorescence patches.

To describe the extent of spatial overlap between IL2Rα and IL15Rα domains, cross-correlation analysis was performed on Cy5 and Alexa-Fluor-488 images obtained simultaneously from double-labeled cells. For a pair of images x and y, the cross-correlation coefficient (C) between the intensity distributions of cell-surface labeling was calculated as:

$$C = \frac{\sum_{i,j}(x_{ij}-\langle x\rangle)(y_{ij}-\langle y\rangle)}{\sqrt{\sum_{i,j}(x_{ij}-\langle x\rangle)^2 \sum_{i,j}(y_{ij}-\langle y\rangle)^2}},$$

where x_{ij} and y_{ij} are fluorescence intensities at pixel coordinates i,j in images x and y, and $\langle x\rangle$, $\langle y\rangle$ are the mean intensities for the total images x and y, respectively. C can vary from –1 (anti-correlated) to 0 (uncorrelated) and 1 (fully correlated).

References

Bene, L., Kanyari, Z., Bodnar, A., Kappelmayer, J., Waldmann, T. A., Vámosi , G. and Damjanovich, L. (2007). Colorectal carcinoma rearranges cell surface protein topology and density in CD4+ T cells. *Biochem. Biophys. Res. Commun.* **361**, 202-207.

Budagian, V., Bulanova, E., Paus, R. and Bulfone-Paus, S. (2006). IL-15/IL-15 receptor biology: a guided tour through an expanding universe. *Cytokine Growth Factor Rev.* **17**, 259-280.

Bulanova, E., Budagian, V., Pohl, T., Krause, H., Durkop, H., Paus, R. and Bulfone-Paus, S. (2001). The IL-15R alpha chain signals through association with Syk in human B cells. *J. Immunol.* **167**, 6292-6302.

Chirifu, M., Hayashi, C., Nakamura, T., Toma, S., Shuto, T., Kai, H., Yamagata, Y., Davis, S. J. and Ikemizu, S. (2007). Crystal structure of the IL-15-IL-15Ra complex, a cytokine-receptor unit presented in trans. *Nat. Immunol.* **8**, 1001-1007.

de Bakker, B. I., de Lange, F., Cambi, A., Korterik, J. P., van Dijk, E. M. H. P., van Hulst, N. F., Figdor, C. G. and Garcia-Parajo, M. F. (2007). Nano-scale membrane organization of the pathogen receptor DC-SIGN mapped by single molecule high resolution fluorescence microscopy. *Chemphyschem* **8**, 1473-1480.

de Lange, F., Cambi, A., Huijbens, R., de Bakker, B. I., Rensen, W., Garcia-Parajo, M. F., van Hulst, N. F. and Figdor, C. G. (2001). Cell biology beyond the diffraction limit: near-field scanning optical microscopy. *J. Cell Sci.* **114**, 4153-4160.

Dubois, S., Mariner, J., Waldmann, T. A. and Tagaya, Y. (2002). IL-15Ralpha recycles and presents IL-15 In trans to neighboring cells. *Immunity* **17**, 537-547.

Dubois, S., Shou, W., Haneline, L. S., Fleischer, S., Waldmann, T. A. and Muller, J. R. (2003). Distinct pathways involving the FK506-binding proteins 12 and 12.6 underlie IL-2-versus IL-15-mediated proliferation of T cells. *Proc. Natl. Acad. Sci. USA* **100**, 14169-14174.

Eicher, D. M. and Waldmann, T. A. (1998). IL-2Ralpha on one cell can present IL-2 to IL-2Rbeta/gammac on another cell to augment IL-2 signaling. *J. Immunol.* **161**, 5430-5437.

Fehniger, T. A. and Caligiuri, M. A. (2001). Interleukin 15, biology and relevance to human disease. *Blood* **97**, 14-32.

Fehniger, T. A., Cooper, M. A. and Caligiuri, M. A. (2002). Interleukin-2 and interleukin-15: immunotherapy for cancer. *Cytokine Growth Factor Rev.* **13**, 169-183.

García-Parajó, M. F., de Bakker, B. I., Koopman, M., Cambi, A., de Lange, F., Figdor, C. G. and van Hulst, N. F. (2005). Near-field fluorescence microscopy: an optical nanotool to study protein organization at the cell membrane. *Nanobiotechnology* **1**, 113-120.

Grabstein, K. H., Eisenman, J., Shanebeck, K., Rauch, C., Srinivasan, S., Fung, V., Beers, C., Richardson, J., Schoenborn, M. A. and Ahdieh, M. (1994). Cloning of a T cell growth factor that interacts with the beta chain of the interleukin-2 receptor. *Science* **264**, 965-968.

Harder, T., Scheiffele, P., Verkade, P. and Simons, K. (1998). Lipid domain structure of the plasma membrane revealed by patching of membrane components. *J. Cell Biol.* **141**, 929-942.

Hori, T., Uchiyama, T., Tsudo, M., Umadome, H., Ohno, H., Fukuhara, S., Kita, K. and Uchino, H. (1987). Establishment of an interleukin 2-dependent human T cell line from a patient with T cell chronic lymphocytic leukemia who is not infected with human T cell leukemia/lymphoma virus. *Blood* **70**, 1069-1072.

Ianoul, A., Grant, D., Rouleau, Y., Bani-Yaghoub, M., Johnston, L. and Pezacki, J. P. (2005). Imaging nanometer domains of β-adrenergic receptor complexes on the surface of cardiac myocytes. *Nat. Chem. Biol.* **1**, 196-202.

Koopman, M., Cambi, A., de Bakker, B. I., Josten, B., Figdor, C. G., van Hulst, N. F. and Garcia-Parajo, M. F. (2004). Near-field scanning optical microscopy in liquid for high resolution single molecule detection on dendritic cells. *FEBS Lett.* **573**, 6-10.

Ku, C. C., Murakami, M., Sakamoto, A., Kappler, J. and Marrack, P. (2000). Control of homeostasis of CD8+ memory T cells by opposing cytokines. *Science* **288**, 675-678.

Lin, J. X., Migone, T. S., Tsang, M., Friedmann, M., Weatherbee, J. A., Zhou, L., Yamauchi, A., Bloom, E. T., Mietz, J., John, S. et al. (1995). The role of shared receptor motifs and common Stat proteins in the generation of cytokine pleiotropy and redundancy by IL-2, IL-4, IL-7, IL-13, and IL-15. *Immunity* **2**, 331-339.

Liparoto, S. F., Myszka, D. G., Wu, Z., Goldstein, B., Laue, T. M. and Ciardelli, T. L. (2002). Analysis of the role of the interleukin-2 receptor gamma chain in ligand binding. *Biochemistry* **41**, 2543-2551.

Marks-Konczalik, J., Dubois, S., Losi, J. M., Sabzevari, H., Yamada, N., Feigenbaum, L., Waldmann, T. A. and Tagaya, Y. (2000). IL-2-induced activation-induced cell death is inhibited in IL-15 transgenic mice. *Proc. Natl. Acad. Sci. USA* **97**, 11445-11450.

Matkó, J., Bodnar, A., Vereb, G., Bene, L., Vámosi, G., Szentesi, G., Szollosi, J., Gaspar, R., Horejsi, V., Waldmann, T. A. et al. (2002). GPI-microdomains (membrane rafts) and signaling of the multi-chain interleukin-2 receptor in human lymphoma/leukemia T cell lines. *Eur. J. Biochem.* **269**, 1199-1208.

Nagy, P., Matyus, L., Jenei, A., Panyi, G., Varga, S., Matkó, J., Szollosi, J., Gaspar, R., Jovin, T. M. and Damjanovich, S. (2001). Cell fusion experiments reveal distinctly different association characteristics of cell-surface receptors. *J. Cell Sci.* **114**, 4063-4071.

Nakamura, Y., Russell, S. M., Mess, S. A., Friedmann, M., Erdos, M., Francois, C., Jacques, Y., Adelstein, S. and Leonard, W. J. (1994). Heterodimerization of the IL-2 receptor beta- and gamma- chain cytoplasmic domains is required for signaling. *Nature* **369**, 330-333.

Nelson, B. H. and Willerford, D. M. (1998). Biology of the interleukin-2 receptor. *Adv. Immunol.* **70**, 1-81.

Rubin, L. A., Kurman, C. C., Biddison, W. E., Goldman, N. D. and Nelson, D. L. (1985). A monoclonal antibody 7G7/B6, binds to an epitope on the human interleukin-2 (IL-2) receptor that is distinct from that recognized by IL-2 or anti-Tac. *Hybridoma* **4**, 91-102.

Sato, N., Patel, H. J., Waldmann, T. A. and Tagaya, Y. (2007). The IL-15/IL-15R on cell surfaces enables sustained IL-15 activity and contributes to the long survival of CD8 memory T cells. *Proc. Natl. Acad. Sci. USA* **104**, 568-593.

Sebestyen, Z., Nagy, P., Horvath, G., Vámosi, G., Debets, R., Gratama, J. W., Alexander, D. R. and Szollosi, J. (2002). Long wavelength fluorophores and cell-by-cell correction for autofluorescence significantly improves the accuracy of flow cytometric energy transfer measurements on a dual-laser benchtop flow cytometer. *Cytometry* **48**, 124-135.

Szöllösi, J., Horejsi, V., Bene, L., Angelisova, P. and Damjanovich, S. (1996). Supramolecular complexes of MHC class I, MHC class II, CD20, and tetraspan molecules (CD53, CD81, and CD82) at the surface of a B cell line JY. *J. Immunol.* **157**, 2939-2946.

Tagaya, Y., Bamford, R. N., DeFilippis, A. P. and Waldmann, T. A. (1996). IL15: a pleiotropic cytokine with diverse receptor/signaling pathways whose expression is controlled at multiple levels. *Immunity* **4**, 329-336.

Vámosi, G., Bodnar, A., Vereb, G., Jenei, A., Goldman, C. K., Langowski, J., Toth, K., Matyus, L., Szollosi, J., Waldmann, T. A. and Damjanovich, S. (2004). IL-2 and IL-15 receptor alpha-subunits are coexpressed in a supramolecular receptor cluster in lipid rafts of T cells. *Proc. Natl. Acad. Sci. USA* **101**, 11082-11087.

van Hulst, N. F., Veerman, J. A., Garcia-Parajo, M. F. and Kuipers, L. (2000). Analysis of individual (macro)molecules and proteins using near-field optics. *J. Chem. Phys.* **112**, 7799-7810.

Vereb, G., Matkó, J., Vámosi, G., Ibrahim, S. M., Magyar, E., Varga, S., Szollosi, J., Jenei, A., Gaspar, R., Jr, Waldmann, T. A. et al. (2000). Cholesterol-dependent clustering of IL-2Ralpha and its colocalization with HLA and CD48 on T lymphoma cells suggest their functional association with lipid rafts. *Proc. Natl. Acad. Sci. USA* **97**, 6013-6018.

Waldmann, T. A. and Tagaya, Y. (1999). The multifaceted regulation of interleukin-15 expression and the role of this cytokine in NK cell differentiation and host response to intracellular pathogens. *Annu. Rev. Immunol.* **17**, 19-49.

Waldmann, T. A., Dubois, S. and Tagaya, Y. (2001). Contrasting roles of IL-2 and IL-15 in the life and death of lymphocytes: implications for immunotherapy. *Immunity* **14**, 105-110.

Yang, X. Y., Jiang, H., Hartmann, W. K., Mitra, G. and Soman, G. (2003). Development of a quantitative antigen-specific cell-based ELISA for the 7G7/B6 monoclonal antibody directed toward IL-2Ralpha. *J. Immunol. Methods* **277**, 87-100.